Journal of Biomolecular NMR **28:** 289–294, 2004.
KLUWER/ESCOM

3D TROSY-HNCA^{coded}CB and TROSY-HNCA^{coded}CO experiments: Triple resonance NMR experiments with two sequential connectivity pathways and high sensitivity

Christiane Ritter, Thorsten Lührs, Witek Kwiatkowski & Roland Riek*
Structural Biology Laboratory, The Salk Institute, 10010 N Torrey Pines Road, La Jolla, CA 92037, U.S.A.

Received 27 June 2003; Accepted 1 September 2003

Key words: biological macromolecules, chemical shift-coding, multidimensional experiments, NMR, triple resonance experiment

Abstract

The concept of chemical shift-coding monitors chemical shifts in multi–dimensional NMR experiments without additional polarization transfer elements and evolution periods. The chemical shifts are coded in the line-shape of the cross-peak through an apparent scalar coupling dependent upon the chemical shift. This concept is applied to the three-dimensional triple-resonance experiment HNCA adding the information of $^{13}C^{\beta}$ or $^{13}C'$ chemical shifts. On average, the proposed TROSY-HNCA^{coded}CB experiment is a factor of 2 less sensitive than the HNCA experiment. However, it contains correlations *via* the chemical shifts of both $^{13}C^{\alpha}$ and $^{13}C^{\beta}$, and provides up to three times higher resolution along the $^{13}C^{\alpha}$ chemical shift axis. Thus, it dramatically reduces ambiguities in linking the spin systems of adjacent residues in the protein sequence during the sequential assignment. The TROSY-HNCA^{coded}CO experiment which is conceptually similar contains correlations *via* the chemical shifts of $^{13}C^{\alpha}$ and ^{13}C' without major signal losses. The proposed triple resonance experiments are applied to a ∼70% ^{2}H, ∼85% ^{13}C,^{15}N labeled protein with a molecular weight of 25 kDa.

Abbreviations: HNCA – amide proton-to-nitrogen-to-alpha-carbon correlation; HNCA^{coded}CB – HNCA with the additional chemical shift of beta-carbons coded in the line-shapes of the cross-peaks along the alpha-carbon frequency; HNCA^{coded}CO – HNCA with the additional chemical shift of carbonyls coded in the line-shapes of the cross-peaks along the alpha-carbon frequency; INEPT – insensitive nuclei enhanced by polarization transfer; NMR – nuclear magnetic resonance; PFG – pulsed field gradient; TROSY – transverse relaxation-optimized spectroscopy; 2D, 3D, 4D – two-dimensional, three-dimensional, four-dimensional; SAR – structure-activity relationships; I-BURP – spin-inversion band-selective uniform-response pure-phase.

Introduction

The introduction of triple-resonance experiments for the sequential assignment of protein polypeptide chains has been a major break-through in the structure determination of protein molecules in aqueous solution (Bax & Grzesiek, 1993; Gardner & Kay, 1998). The potential of this approach has been further extended (Riek et al., 2000) by the introduction of the TROSY-technique (Pervushin et al., 1997) into triple resonance experiments (Salzmann et al., 1998; Riek, 2003). Using this approach, the backbone assignments of a multimeric protein with a molecular weight of 110 kDa (Salzmann et al., 1999) and of a monomeric protein with 736 amino acid residues in length (Tugarinov et al., 2002) have been achieved.

However, the successful backbone assignment of large proteins requires expensive preparation of perdeuterated ^{13}C,^{15}N labeled protein samples and lengthy NMR measuring time of several weeks. With the advent of NMR-based structural genomics (Montelione et al., 2000) and SAR by NMR (Shuker et al., 1996), major challenges to be focused on are (i) the reduction of NMR-data collection time needed to obtain chemical shift assignments of proteins and (ii) the straightforward production of labeled proteins. Marley et al. recently presented a rapid and efficient

*To whom correspondence should be addressed: E-mail: riek@sbl.salk.edu

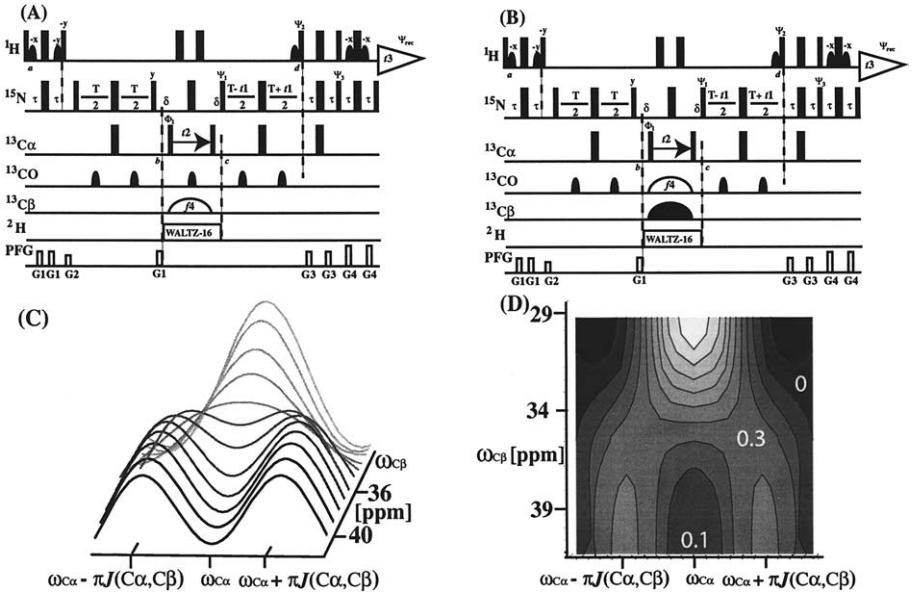

Figure 1. Experimental scheme for the (A) TROSY-HNCA^{coded}CB experiment and (B) TROSY-HNCA^{coded}CO experiment for deuterated and protonated ^{13}C,^{15}N-labeled proteins. (C) Stacked-trace plot showing the relation between the $^{13}C^{\beta}$ chemical shift and the peak shape in the transformed spectrum of a $^{13}C^{\alpha}$ moiety in a 85% ^{13}C,^{15}N-labeled protein. (D) Contour plot of the relation between the $^{13}C^{\beta}$ chemical shift and the peak shape in the transformed spectrum. (A and B): The radio-frequency pulses on ^{1}H, ^{15}N, $^{13}C^{\alpha}$, $^{13}C^{\beta}$, $^{13}C'$, ^{2}H or $^{1}H^{\alpha}$ were applied at 4.8, 119, 55, 29, 175, 3.8 and 4.8 ppm, respectively. The narrow and wide black bars indicate non-selective 90° and 180° pulses, respectively. On the line marked $^{13}CO^{\beta}$, the sine bell shape designated with $f4$ indicates a selective 180° pulse with a Gaussian shape truncated at 5% and a duration of 0.7 ms. On the line marked ^{13}CO, a sine bell shape designated with $f4$ indicates a selective 180° pulse with a Gaussian shape truncated at 5%, a duration of 1.3 ms and applied with an off-resonance shift of −2.5 ppm. On the line marked $^{13}C^{\beta}$, the filled sine bell shape indicates a selective 180° pulse with a I-BURP-1 shape, a duration of 1.1 ms and an off-resonance shift of −2 ppm. On the line marked ^{13}CO, a filled sine bell shapes indicate selective 180° pulses with a Gaussian shape truncated at 5% and a duration of 0.08 ms. The length of the softpulses have been optimized for a magnetic field strength of 700 MHz ^{1}H frequency. The line marked PFG indicates durations and amplitudes of sine shaped pulse magnetic field gradients applied along the z-axis: G_1: 0.8 ms, 15 G/cm, G_2: 0.8 ms, 9 G/cm; G_3: 0.8 ms, 22 G/cm; G_4: 0.8 ms, 22 G/cm. The delays are $\tau = 2.7$ ms, $T = 30$ ms, $\sigma = 0.5$ ms. The phase cycle is ψ_1 = y,-y,x,-x, ψ_2 = -y, ψ_3 = -y, Φ_1 = 4 x, 4 -x and Φ_{rec} = y,-y,-x,x,-y,y,x,-x. All other radio frequency pulses are applied either with phase x or as indicated above the pulses. In the $^{15}N(t_1)$ dimension a phase-sensitive spectrum is obtained by recording a second FID for each increment of t_1, with ψ_1 = y, -y, -x, x, ψ_2 = y, ψ_3 = y and the data is processed as described by Kay et al. (1992). Quadrature detection in the $^{13}C^{\alpha}(t_2)$ dimension is achieved by the States-TPPI method (Marion et al., 1989) applied to the phase Φ_1. Between time points b and c the timing of the radio frequency pulses of the different nuclei have been implemented in a parallel manner to achieve an initial $t_2 = 0$. The water magnetization stays aligned along the +z-axis throughout the experiment by the use of water flip-back 90° pulses with a duration of 1 ms and a Gaussian shape truncated at 5% indicated by sine bell shapes on the line ^{1}H (Grzesiek and Bax, 1993). For ^{2}H-decoupling, WALTZ-16 (Shaka et al., 1983) is used with a field strength of 2.5 kHz. For protonated proteins, the radio-frequency line labeled with ^{2}H should be removed. (C) Stacked trace plot at 1 ppm interval generated by Fourier transformation of $0.85\,(1-a(\omega_{C\beta})\,\cos[\omega_S t]\,\cos[\pi\,{}^1J(I,S)t]+a(\omega_{C\beta})\,\cos[\omega_S t]$ and $a(\omega_{C\beta}) = \exp[-(\omega_{c\beta,max}-\omega_{c\beta})^2\,\ln[20]/(0.5(\omega_{c\beta,max}-\omega_{c\beta,min}))^2]$ with $\omega_{c\beta,max} = 29$ ppm and $\omega_{c\beta,min} = 42$ ppm and $t_{max} = 1/{}^1J(I,S)$ (Kwiatkwoski and Riek, 2003). (D) The contour plot is generated using the parameters in (C). The shading of the contour plot is related to the intensity in steps of 0.1 (1 is the maximal relative intensity). A potential distortion of the line shape due to Bloch-Siegert effect is not included in the simulations.

approach for the preparation of isotopically labeled proteins in *E. coli* (Marley et al., 2001). Their approach provides a fourfold to eightfold reduction in isotope costs, but also allows for a straightforward adaptation from protein-specific expression protocols that use rich media. This is of particular interest when deuterated proteins are needed, because standard labeling protocols which require prolonged growth in deuterated media often result in a severe decrease or a complete loss of protein expression (Gardner and Kay, 1998; Marley et al., 2001; C. Ritter, T. Lührs, R. Riek, K. Baker and S. Choe, unpublished observations). The drawback of this labeling method is the relatively low level of incorporation of ^{15}N and ^{13}C to about 85% and deuteration to about 70%. This low deuteration level dramatically reduces the sensitivity of the triple resonance experiments. Therefore, the major need for NMR-based structural genomics and

SAR using such expression methods are novel triple resonance experiments with high sensitivity and high quality of information for sequential correlation.

Here we present the TROSY-HNCA^{coded}CB and TROSY-HNCA^{coded}CO experiments, which fit the demanded criteria. These experiments are TROSY-based HNCA-type experiments that contain in addition to the $^{13}C^{\alpha}$chemical shifts the $^{13}C^{\beta}$or $^{13}C'$ chemical shift information coded in the $^{13}C^{\alpha}$-multiplet structure based on the concept of chemical shift-coding introduced recently (Kwiatkowski and Riek, 2003). In this approach, chemical shifts in multi–dimensional NMR experiments are monitored without additional polarization transfer elements and evolution periods. Instead, additional chemical shifts are coded in the line-shape of the cross-peaks through a chemical shift-dependent apparent scalar coupling active during an established evolution period.

The TROSY-HNCA^{coded}CB experiment is based on the TROSY-HNCA experiment (Eletski et al., 2001) with one minor but pivotal difference during the $^{13}C^{\alpha}$ evolution period, t_2 (Figure 1A). During the frequency labeling period t_2 the $^{13}C^{\alpha}$ magnetization evolves under its chemical shift and the scalar coupling $^1J(^{13}C^{\alpha},^{13}C^{\beta})$ with a size of ∼35 Hz. However, the 180° soft pulse on $^{13}C^{\beta}$ controls the extent of the refocusing of the $^1J(^{13}C^{\alpha},^{13}C^{\beta})$ coupling. This soft pulse is on resonance at the high-field edge of the $^{13}C^{\beta}$ chemical shift range (excluding alanine $^{13}C^{\beta}$s) and contains a Gaussian excitation profile $a(\omega(^{13}C^{\beta}))$. The profile decreases approximately linearly over the $^{13}C^{\beta}$ chemical shift range resulting in 100% inversion at 29 ppm to 3% inversion at 41 ppm and is given by

$$a(\omega(^{13}C^{\beta})) = \exp[-(\omega_{C\beta,\max} - \omega_{C\beta})^2 \ln(100/C)/ (0.5(\omega_{C\beta,\max} - \omega_{C\beta,\min}))^2], \quad (1)$$

$C = 5$, $\omega_{C\beta,\max} = 29$ ppm. Thus, the extent of the refocusing of $^1J(^{13}C^{\alpha},^{13}C^{\beta})$ and the multiplet pattern of the cross-peak in the spectrum along the $^{13}C^{\alpha}$ dimension depend on the corresponding $^{13}C^{\beta}$ chemical shift, leading to chemical shift dependent apparent scalar couplings. As a result, the $^{13}C^{\beta}$ chemical shift is encoded in the line-shape of the cross-peak along the $^{13}C^{\alpha}$dimension (Kwiatkowski and Riek, 2003). With a $t_{2\max} \approx 1/^1J(^{13}C^{\alpha}, ^{13}C^{\beta})$, the cross-peak appears in the spectrum along the $^{13}C^{\alpha}$ frequency as a doublet with a residual apparent scalar coupling of

$$^{residual}J(^{13}C^{\alpha},^{13}C^{\beta}) \approx [1 - a(\omega(^{13}C^{\beta}))] \; ^1J(^{13}C^{\alpha},^{13}C^{\beta}) \quad (2)$$

(Figures 1C and 1D; Kwiatkowski and Riek, 2003). Typically, a $t_{2\max}$ of 27–35 ms is used in the HNCA^{coded}CB experiment. The coherence flow can thus be described as follows:

$$^1H(i) \rightarrow {}^{15}N(i) \begin{cases} \nearrow {}^{13}C^{\alpha}(i)[t_2] \cos[\pi {}^{residual}J(^{13}C^{\alpha}(i),^{13}C^{\beta}(i))t_2] \\ \searrow {}^{13}C^{\alpha}(i-1)[t_2] \cos[\pi {}^{residual}J(^{13}C^{\alpha}(i-1),^{13}C^{\beta}(i-1))t_2] \end{cases} \searrow \nearrow {}^{15}N(i)[t_2] \rightarrow {}^1H(i)[t_3].$$

In addition to the TROSY-HNCA^{coded}CB experiment we have also proposed the TROSY-HNCA^{coded}CO experiment, which is similar to the TROSY-HNCA^{coded}CB experiment with the following difference during the $^{13}C^{\alpha}$ evolution period t_2 (Figure 1): The $^1J(^{13}C^{\alpha},^{13}C')$ scalar coupling with a size of ∼55 Hz evolves, whereas the $^1J(^{13}C^{\alpha},^{13}C^{\beta})$ coupling is suppressed applying an I-BURP-1 pulse for a duration of 1.1 ms on resonance at 27 ppm. The 180° Gaussian soft pulse on $^{13}C'$ controls the extent of the refocusing of the $^1J(^{13}C^{\alpha},^{13}C')$ coupling. This soft pulse is on resonance at the high-field limit of the $^{13}C'$ chemical shift range (172.5 ppm) and contains a Gaussian excitation profile $a(\omega(^{13}C')) = \exp[-(\omega_{C'\max} - \omega_{C\beta})^2 \ln(100/C) \quad /(0.5(\omega_{C',\max} - \omega_{C',\min}))^2$ with $C = 5$ and decreases approximately linearly over the $^{13}C'$ chemical shift range, resulting in 100% inversion at 172.5 ppm to 3% inversion at 178.5 ppm. Thus, with a $t_{2\max} < 1/^1J(^{13}C^{\alpha},^{13}C')$ the cross-peak appears in the spectrum along the $^{13}C^{\alpha}$ frequency as a doublet with a residual apparent scalar coupling $^{residual}J(^{13}C^{\alpha},^{13}C') \approx [1-a(\omega(^{13}C'))]\,^1J(^{13}C^{\alpha},^{13}C')$ (Kwiatkowski and Riek, 2003). The evolution of $^1J(^{13}C^{\alpha},^{13}C^{\beta})$ scalar couplings is not perfectly refocused for $^{13}C^{\beta}$ chemical shifts in the range between 36 and 42 ppm because of the inversion profile of the I-BURP-1 soft pulse and hence an evolution time $t_{2\max}$ of 18–22 ms is suggested. Furthermore, the extraction of the $^{13}C'$ chemical shift from the line-shape is ambiguous due to the partial evolution of some of the $^1J(^{13}C^{\alpha},^{13}C^{\beta})$ scalar couplings.

In Figure 2, we show strips and cross-sections from a 3D TROSY-HNCA^{coded}CB spectrum of ∼70% ^{2}H-, ∼85% ^{13}C,^{15}N-labeled pHET-s*(1-227), which has a molecular weight of 25 kDa and a rotational correlation time τ_c of ∼17 ns. The sample was prepared using the method of Marley et al. (2001). As in the HNCA experiment, the cross-peak with the larger volume usually corresponds to intra-residue correlations between the intraresidual $^{13}C^{\alpha}$ carbons and the ^{15}N-^{1}H moiety, and the weaker cross-peak usually represents the sequential correlations. Taking the overall position of

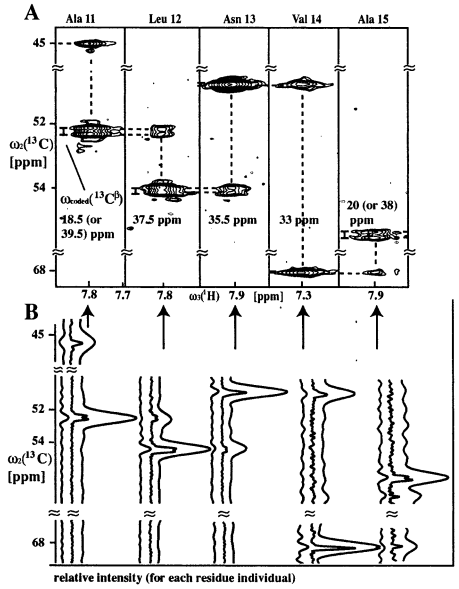

Figure 2. (A) Strips of the 3D TROSY-HNCA^{coded}CB spectrum of pHET-s*(1–227). (B) Comparison of the corresponding cross-sections along the $\omega_2(^{13}C)$ dimension of TROSY-HNCA^{coded}CB experiment (middle lines), TROSY-HNCA experiment (left lines), and TROSY-ct-HNCA experiment (right lines). The sequential connectivities and assignments are indicated. The $^{13}C^{\beta}$ chemical shifts specified have been extracted from the peak pattern along $\omega_2(^{13}C^{\alpha})$ (Kwiatkowski and Riek, 2003). Chemical shift ambiguities listed are due to the use of the soft-pulse of $^{13}C^{\beta}$ on-resonance at 29 ppm (Figure 1). The spectra are recorded at 700 MHz ^{1}H frequency at 28 °C with a 2.5 mM sample of 70% ^{2}H-, 85% ^{13}C,^{15}N-labeled pHET-s*(1–227) in a mixed solvent of 95% H_2O/5% D_2O at pH 7. The following parameter settings are used for the 3D TROSY-HNCA^{coded}CB experiment: data size $35(t_1)$*$175(t_2)$*$1024(t_3)$ complex points; $t_{1\,max}(^{15}N)$ = 24 ms, $t_{2\,max}$ ($^{13}C^{\alpha}$) = 30.5 ms, $t_{3\,max}(^{1}H)$ = 75.6 ms. The data set is zero-filled to 128*2048*1024 complex points; 8 scans per increment are acquired. 3D TROSY-HNCA experiment: $35(t_1)$*$44(t_2)$*$1024(t_3)$ complex points; t_{max} (^{15}N) = 24 ms, $t_{2\,max}$ ($^{13}C^{\alpha}$) = 30/4 ms, $t_{3\,max}(^{1}H)$ = 75.6 ms. The data set is zero-filled to 128*2048*1024 complex points; 32 scans per increment are acquired. 3D TROSY-ct-HNCA experiment: $35(t_1)$*$175(t_2)$*$1024(t_3)$ complex points; $t_{1\,max}$ (^{15}N)= 24 ms, $t_{2\,max}$ ($^{13}C^{\alpha}$) = 26.5 ms, $t_{3\,max}$(1H) = 75.6 ms. The data set is zero-filled to 128*2048*1024 complex points; 8 scans per increment are acquired. The experiments are measured for equal times.

the $^{13}C^{\alpha}$ cross-peak as a starting point, the sequential connectivities are then reinforced through the multiplet pattern of the $^{13}C^{\alpha}$ cross-peak (Figure 2). Only when the multiplet pattern of a sequential cross-peak fits with the pattern of an intra-residue cross-peak, the sequential connectivity is confirmed. The sequential correlation is therefore supported by two independent correlations, the $^{13}C^{\alpha}$ and $^{13}C^{\beta}$ chemical shifts. This line-shape comparison significantly reduces ambiguities in linking the spin systems of adjacent residues in the protein sequence during the sequential assignment process. In addition, the $^{13}C^{\beta}$ chemical shift information can be extracted from the line-shape using the program INFIT (Szyperski et al., 1992) to obtain the apparent scalar coupling and the Equation 2 to calculate the chemical shift. This is important for an unambiguous mapping of the connected strip-fragments onto the amino acid sequence. The precision of the $^{13}C^{\beta}$ chemical shifts obtained using this method is approximately ±2 ppm when compared with the corresponding chemical shifts determined from the TROSY-HNCACB experiment (data not shown). The accuracy depends on the maximal evolution time $t_{2\,max}$, the size of the scalar coupling $^{1}J(^{13}C^{\alpha},^{13}C^{\beta})$ ∼35 Hz, the spectral range (in Hz) of the $^{13}C^{\beta}$ chemical shifts, which has to be covered by the shoulder of the inversion profile of the soft-pulse (Kwiatkowski and Riek, 2003), and peak shape distortion due to long range ^{2}H isotope effects. In order to maximize the $^{13}C^{\beta}$ chemical shift resolution to the above mentioned ±2 ppm, we chose an inversion profile covering 29–41 ppm (see above). Due to the symmetry of the softpulse, a $^{13}C^{\beta}$ chemical shift of 19 ppm of alanine and a $^{13}C^{\beta}$ with a chemical shift of 39 ppm display the same splitting (Figure 2). Fortunately, the combination of a cross peak at a $^{13}C^{\alpha}$ chemical shift of ∼ 53 ppm with an almost full splitting (∼ 35 Hz) can be assigned unambiguously to an alanine residue. Similarly, the cross-peaks with a full splitting of 35 Hz and a $^{13}C^{\alpha}$ chemical shift larger than 56 ppm belong to serine or threonine residues, although the apparent residual scalar coupling of 35 Hz indicates only that the $^{13}C^{\beta}$ chemical shift is 41 ppm or larger. The achieved resolution of ±2 ppm is sufficient for the identification of amino acid residues, since the residue-specific $^{13}C^{\beta}$ chemical shifts have a standard deviation of ±2.5 ppm (BMRB data base).

The spectral resolution of a TROSY-HNCA is limited by the short $t_{2\,max}$ of typically only 8 ms due to the evolution of $^{1}J(^{13}C^{\alpha},^{13}C^{\beta})$. Since this evolution of $^{1}J(^{13}C^{\alpha},^{13}C^{\beta})$ is desired in the proposed TROSY-HNCA^{coded}CB experiment, long $t_{2\,max}$ of 27–35 ms can be used. This increases the ^{13}C spectral resolution three-to-four fold when compared to a TROSY-HNCA experiment. Similarly high resolution along the $^{13}C^{\alpha}$ dimension has been achieved in the TROSY-ct-HNCA experiment (Salzmann et al., 1999a) using a constant time period of 27 ms, accompanied however, with a dramatic signal loss (Figure 2B). Hence, Matsuo and coworkers (1996) proposed a $^{13}C^{\beta}$-decoupled

HNCA experiment, which contains the same high resolution, but is more sensitive than the corresponding ct-version. Technically, the $^{13}C^{\beta}$-decoupled TROSY-HNCA experiment is very similar to the proposed TROSY-HNCA^{coded}CB differing only in the decoupling scheme (in the paper of Matsuo et al. TROSY was not yet established and therefore not implemented). As demonstrated by Matsuo and coworkers the complete decoupling of the $^{1}J(^{13}C^{\alpha},^{13}C^{\beta})$ scalar couplings in the $^{13}C^{\beta}$-decoupled HNCA experiment enhances the signal intensity of the non-glycine cross peaks between 1–1.5 (on average 1.25) when compared with a non-decoupled experiment using the same t_{max} (Matsuo et al., 1996: Figure 2). The theoretically predicted factor of 2 in signal enhancement could not be achieved, probably due to the extensive and demanding decoupling scheme used. In contrast, the measured sensitivity gain of 0.9–2 (on average 1.45) for the TROSY-HNCA^{coded}CB when compared with the non-decoupled experiment using the same t_{max} (data measured with ^{13}C,^{15}N-labeled ubiquitin, but not shown) are close to the expected gain due to the simple (partial) decoupling scheme used. Furthermore, the $^{13}C^{\beta}$ chemical shift is measured concurrently.

In a comparison with the conventional TROSY-based HNCA experiment, the TROSY-HNCA^{coded}CB spectrum is a factor of 1.2–3 less sensitive (Figure 2B). The origin of this sensitivity loss is the splitting of the cross-peak into the $^{13}C^{\beta}$-chemical shift dependent multiplet structure and the additional transverse relaxation occurring during the three-fold longer t_2. On the other hand, the TROSY-HNCA^{coded}CB spectrum is a factor of 2–3 more sensitive than the TROSY-ct-HNCA experiment (Figure 2B), since the TROSY-HNCA^{coded}CB experiment is measured in a non-constant time manner and also the partial carbon labeling reduces the sensitivity of the TROSY-ct-HNCA due to the opposite phase of $^{13}C^{\alpha}$-$^{13}C^{\beta}$ and $^{13}C^{\alpha}$-$^{12}C^{\beta}$ moieties. Similar improvement in sensitivity could be seen, when compared with a TROSY-HNCACB experiment. For example, 98% of the expected intraresidual and 85% of the expected sequential $^{13}C^{\alpha}$ crosspeaks could be observed in the TROSY-HNCA^{coded}CB, but only 75% of the intraresidual and 20% of the sequential $^{13}C^{\alpha}$ crosspeaks were observed in the TROSY-HNCACB experiment.

To reduce the ambiguities further in the backbone assignment of large proteins we suggest the additional use of the TROSY-HNCA^{coded}CO experiment. The TROSY-HNCA^{coded}CO is an HNCA-type experiment that contains the $^{13}C'$ chemical shift information coded in the $^{13}C^{\alpha}$-multiplet structure of the $^{13}C^{\alpha}$ crosspeaks using the concept of chemical shift-coding. Figure 3A shows cross-sections from a 3D TROSY-HNCA^{coded}CO experiment and a 3D TROSY-HNCA^{coded}CB experiment displaying significantly different splittings of the same $^{13}C^{\alpha}$ crosspeak. Therefore, the two spectra contain complementary information about the same sequential correlations. In the cross-section of the TROSY-HNCA^{coded}CB experiment, the splitting is due to the corresponding $^{13}C^{\beta}$ chemical shift, and in the TROSY-HNCA^{coded}CO experiment the observed splitting is due to the $^{13}C'$ chemical shift.

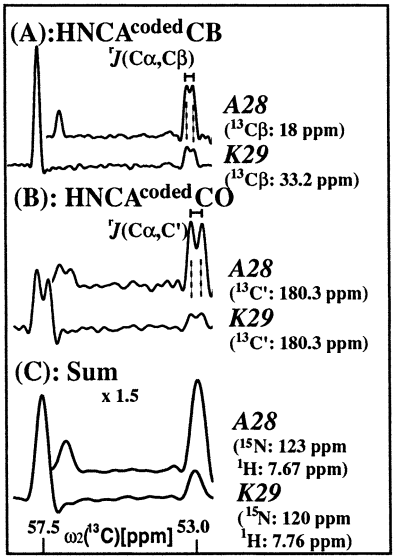

Figure 3. Cross-sections of ^{13}C,^{15}N-labeled ubiquitin of the (A) TROSY-HNCA^{coded}CB, (B) TROSY-HNCA^{coded}CO experiment and (C) combination of both spectra. The sequential connectivities are marked. For comparison, the cross sections have been scaled to the same noise for each strip individually. The TROSY-HNCA^{coded}CO spectrum is recorded at 700 MHz ^{1}H frequency at 20 °C with a 0.8 mM uniformly ^{13}C,^{15}N-labeled ubiquitin in a mixed solvent of 95% H_2O/5% D_2O at pH 6.5. The following parameter settings are used: data size $16(t_1)*110(t_2)*1024(t_3)$ complex points; $t_{1\,max}(^{15}N)$ = 11 ms, $t_{2\,max}$ ($^{13}C^{\alpha}$) = 20 ms, $t_{3\,max}(^{1}H)$ = 75.6 ms. The data set is zero-filled to 64*1024*1024 complex points; 4 scans per increment are acquired with a total measurement time of 4 h. The parameters of the TROSY-HNCA^{coded}CB spectrum are $16(t_1)*175(t_2)*1024(t_3)$ complex points; $t_{1\,max}(^{15}N)$ = 11 ms, $t_{2\,max}$ ($^{13}C^{\alpha}$) = 30 ms, $t_{3\,max}(^{1}H)$ = 75.6 ms. The data set is zero-filled to 64*2048*1024 complex points; 4 scans per increment are acquired with a total measurement time of 6 h.

Another intriguing feature of the proposed concept of HNCA-coded experiments is the possibility to generate a spectrum of higher sensitivity using the same data sets. This can be achieved by a partial transform-

ation of the HNCA^{coded}CB experiment using the first 8–13 ms in t_2, or when both experiments are collected, by the combination of the HNCA^{coded}CB and the HNCA^{coded}CO experimental data collections into one spectrum using the first 8–11 ms in t_2 of each (Figure 3C). With such a transformation, the chemical shift information of $^{13}C^{\beta}$ and $^{13}C'$ are largely suppressed, and a significant sensitivity gain is achieved due to less relaxation during t_2. This feature is particularly important for observing cross-peaks with very low sensitivity.

In summary, the HNCA experiment, which links resonances of backbone amide groups with their intra- and inter-residue $^{13}C^{\alpha}$frequencies, is the most sensitive triple-resonance NMR experiment for the sequential assignment of proteins (Bax and Grzesiek, 1993; Gardner and Kay, 1998). However, in the HNCA spectrum of proteins chemical shift degeneracy of $^{13}C^{\alpha}$ nuclei often arises because of limited resolution due to the $^{1}J(^{13}C^{\alpha},^{13}C^{\beta})$ scalar couplings, which often prevents unambiguous correlations between ^{15}N-^{1}H groups. Therefore, additional experiments like the HNCACB or the HNCACO are usually required, which correlate sequentially adjacent ^{15}N-^{1}H groups *via* the $^{13}C^{\beta}$ or $^{13}C'$ frequencies (Yang and Kay, 1999; Wittekind and Muller, 1993). Drawbacks of all these experiments are the reduced intrinsic sensitivity and the requirement to record a multitude of NMR datasets. For example, the HNCACB experiment of a 20 kDa ^{13}C,^{15}N-labeled protein is one order of magnitude less sensitive than the HNCA (Sattler et al., 1999). Signal losses of 5–10 fold are observed for the 25 kDa protein pHET-s(1–227), which was ∼70% ^{2}H, ∼85% ^{13}C,^{15}N labeled in a cost-effective and straightforward approach. It is therefore of keen interest to develop triple-resonance experiments with a similar sensitivity as the TROSY-HNCA but with a much higher quality and quantity of information for sequential correlations. The TROSY-HNCA^{coded}CB and TROSY-HNCA^{coded}CO experiments fit these criteria. Both experiments contain additional information, since the $^{13}C^{\beta}$ or $^{13}C'$ chemical shift is coded in the $^{13}C^{\alpha}$-multiplet structure. Thus, the TROSY-HNCA^{coded}CB and TROSY-HNCA^{coded}CO experiments presented here improve upon the standard triple-resonance experiments in both sensitivity and information content when applied to large proteins prepared in a cost-effective and straightforward way. Therefore, we recommend both experiments for use in obtaining sequence specific chemical shift assignments in an efficient manner.

Acknowledgements

Financial support was obtained from the F.C. Berger Foundation, the Auen Foundation and the National Institute of Health. We thank Dr C.R. Grace and Dr K. Baker for careful reading.

References

Bax, A. and Grzesiek, S. (1993) *Acc. Chem. Res*., **26**, 131–138.
Eletski, A., Kienhofer, A. and Pervushin, K. (2001) *J. Biomol. NMR*, **20**, 177–180.
Gardner, K.H. and Kay, L.E. (1998) *Annu. Rev. Biophys. Biomol. Struct.*, **27**, 357–406.
Grzesiek, S. and Bax, A. (1992) *J. Magn. Reson.*, **96**, 432–440.
Grzesiek, S. and Bax, A. (1992) *J. Am. Chem. Soc.*, **114**, 6291–6293.
Grzesiek, S. and Bax, A. (1993) *J. Am. Chem. Soc.*, **115**, 12593–12594.
Kay, L.E., Ikura, M., Tschudin, R. and Bax, A. (1990) *J. Magn. Reson.*, **89**, 496–514.
Kay, L.E., Keifer, P. and Saarinen, T. (1992) *J. Am. Chem. Soc.*, **114**, 10663–10665.
Kwiatkowski, W. and Riek, R. (2003) *J. Biomol. NMR*, **25**, 281–290.
Marion, D., Ikura, K., Tschudin, R. and Bax, A. (1989) *J. Magn. Reson.*, **85**, 393–399.
Marley, J., Lu, M. and Bracken, C. (2001) *J. Biomol. NMR*, **20**, 71–75.
Matsuo, H., Kupce, E., Li, H. and Wagner, G. (1996) *J. Magn. Reson. B*, **113**, 91–96.
Montelione, G.T., Zheng, D., Huang, Y.J., Gunsalus, K.C. and Szyperski, T. (2000) *Nat. Struct. Biol.*, **7**, 982–985.
Pervushin, K., Riek, R., Wider, G. and Wüthrich, K. (1997) *Proc. Natl. Acad. Sci. USA*, **94**, 12366–12371.
Riek, R. (2003) *Methods and Principles in Medical Chemistry*, O. Zerbe (Ed.), Vol. 16, pp. 227–241.
Riek, R., Pervushin, K. and Wüthrich, K. (2000) *Trends Biochem. Sci.*, **25**, 462–468.
Salzmann, M., Pervushin, K., Wider, G., Senn, H. and Wüthrich, K. (1998) *Proc. Natl. Acad. Sci. USA*, **95**, 13585–13590.
Salzmann, M., Pervushin, K., Wider, G., Senn, H. and Wüthrich, K. (1999a) *J. Biomol. NMR*, **14**, 85–88.
Salzmann, M., Wider, G., Pervushin, K., Senn, H. and Wüthrich, K. (1999b) *J. Am. Chem. Soc.*, **121**, 844–848.
Sattler, M., Schleucher, J. and Griesinger, C. (1999) *Prog. Nucl. Magn. Reson. Spectr.*, **34**, 93–158.
Shaka, A.J., Keeler, J., Frenkiel, T. and Freeman, R. (1983) *J. Magn. Reson.*, **52**, 335–338.
Shuker, S.B., Hajduk, P.J., Meadows, R.P. and Fesik, S.W. (1996) *Science*, **274**, 1531–1534.
Szyperski, T., Guntert, P., Otting, G. and Wüthrich, K. (1992) *J. Magn. Reson*, **99**, 552–560.
Tugarinov, V., Muhandriran, P., Ayed, A. and Kay, L. (2002) *J. Am. Chem. Soc.*, **28**, 10025–10035.
Wittekind, M. and Muller, L. (1993) *J. Magn. Reson.*, **B 101**, 201–205.
Yang, D. and Kay, L.E. (1999) *J. Am. Chem. Soc.*, **121**, 2571–2575.
Zuiderweg, E.R. (2002) *Biochemistry*, **41**, 1–7.